World Academy of Science, Engineering and Technology
International Journal of Geological and Environmental Engineering
Vol:13, No:5, 2019

Seismic Performance of Slopes Subjected to Earthquake Mainshock Aftershock Sequences

Alisha Khanal, Gokhan Saygili

***Abstract*—**It is commonly observed that aftershocks follow the mainshock. Aftershocks continue over a period of time with a decreasing frequency and typically there is not sufficient time for repair and retrofit between a mainshock–aftershock sequence. Usually, aftershocks are smaller in magnitude; however, aftershock ground motion characteristics such as the intensity and duration can be greater than the mainshock due to the changes in the earthquake mechanism and location with respect to the site. The seismic performance of slopes is typically evaluated based on the sliding displacement predicted to occur along a critical sliding surface. Various empirical models are available that predict sliding displacement as a function of seismic loading parameters, ground motion parameters, and site parameters but these models do not include the aftershocks. The seismic risks associated with the post-mainshock slopes ('damaged slopes') subjected to aftershocks is significant. This paper extends the empirical sliding displacement models for flexible slopes subjected to earthquake mainshock-aftershock sequences (a multi hazard approach). A dataset was developed using 144 pairs of as-recorded mainshock-aftershock sequences using the Pacific Earthquake Engineering Research Center (PEER) database. The results reveal that the combination of mainshock and aftershock increases the seismic demand on slopes relative to the mainshock alone; thus, seismic risks are underestimated if aftershocks are neglected.

***Keywords*—**Seismic slope stability, sliding displacement, mainshock, aftershock, landslide, earthquake.

I. Introduction

AN earthquake is a sudden and violent shaking of the ground. The most common causes are the movement of tectonic plates beneath Earth's crust, volcanic action, and human activities such as hydraulic fracturing and deep injection. Depending upon the intensity and duration characteristics, earthquakes can have devastating effects on both human lives and the infrastructure. Generally, an earthquake is not a stand-alone event. Mainshocks are usually preceded and/or followed by a number of foreshocks and/or aftershocks of smaller magnitude.

Earthquakes can trigger landslides that can significantly damage the infrastructure. An earthquake-induced landslide is defined as the downward or upward movement of slope forming materials due to seismic activity. There have been numerous studies focusing on the behavior of slopes during an earthquake. However, the vast majority of these studies consider earthquake as a single event, i.e., they do not account for the entire mainshock–aftershock sequence.

The seismic performance and collapse vulnerability considering mainshock–aftershock sequences have been studied for reinforced concrete frame buildings [13], [7], [6], wood frame structures [5], [25] and steel frame buildings [18], [11], [21], [17]. To date, the occurrence of aftershocks (i.e., multi-hazard approach) has not been included in the assessment of seismic performance of earth slopes. In the geotechnical earthquake engineering literature, there is a knowledge gap regarding the evaluation of the seismic performance of earth slopes subjected to multiple earthquakes (i.e., mainshock– aftershock sequences).

The combination of a mainshock and aftershock increases the seismic demand on slopes relative to the mainshock alone; thus, seismic risks may be underestimated if aftershocks are neglected. The main objective of this research is to provide an improved assessment of risks associated with the seismic performance of earth slopes subjected to earthquake mainshock-aftershock sequences. In this study, the impacts of strength degradation on the yield acceleration of post-mainshock slopes subjected to aftershocks are studied and a case study is demonstrated to explain the effects of aftershocks on the seismic performance of post-mainshock flexible sliding masses.

II. Research Workflow

The goal of this research is to improve the existing empirical sliding displacement models for flexible slopes subjected to earthquake mainshock-aftershock sequence. This objective requires that dynamic response and sliding displacement analyses are performed using a large and high-quality dataset for strong motion records.

A dataset was developed for as-recorded mainshock–aftershock sequences using the Next Generation Attenuation (NGA) strong motion database of the PEER center [12]. In order to exclude structural dynamics, the ground motion records only from instruments located in ground level, basement, or free field were considered. Mainshock and aftershock sequences only from the same stations were used. The initial dataset included 144 strong motion pairs of mainshock-aftershock sequence. As shown in Fig. 1, the strong motion data include mainshocks ranging from M_w = 5.6 to 7.6 and aftershocks ranging from M_w = 4.2 to 7.1. The shear wave velocities were between 179 m/s to 1222 m/s, which corresponds to site classes B to E according to the preferred NEHRP site classification [4]. Most of the mainshocks with M_w > 7.5 did not have aftershock records in the PEER database. Although very rare, it makes the database

Alisha Khanal is with The University of Texas at Tyler, Tyler, TX 75701 USA (corresponding author, phone: 972-948-7530; e-mail: akhanal@patriots.uttyler.edu).

Gokhan Saygili, is with The University of Texas at Tyler, Tyler, TX 75701 USA (e-mail: gsaygili@uttyler.edu).

incomplete for strong aftershocks. The distribution of earthquake magnitude with respect to the distance is shown in Fig. 1 for both mainshocks and aftershocks, respectively.

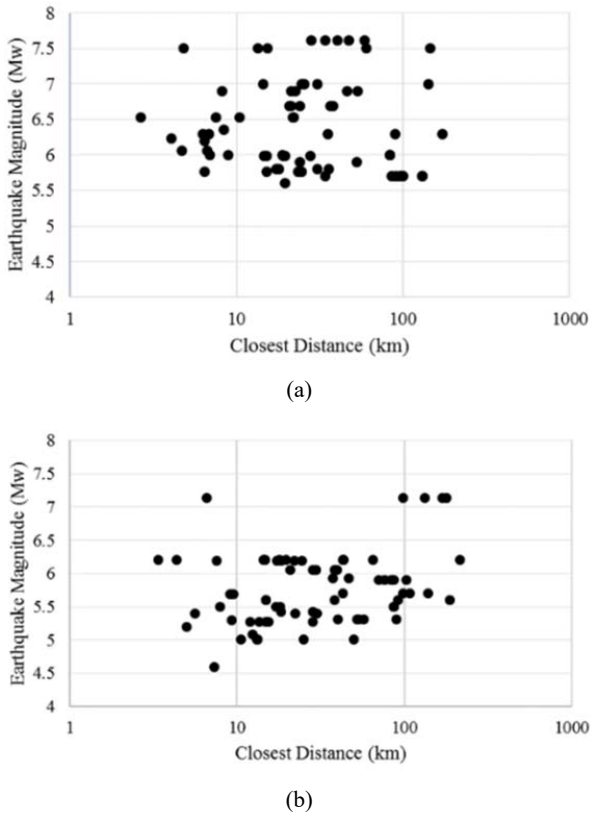

Fig. 1 Earthquake magnitude distribution with respect to closest distance for selected (a) mainshocks and (b) aftershocks

The dynamic response of rigid sliding masses is negligible and can be ignored. However, the dynamic response must be taken into account on deeper and softer sliding masses (i.e., flexible sliding masses) for the estimation of seismic demand. Vrymoed and Calzascia [23] and recently Rathje and Bray [14], showed that dynamic response analyses using one-dimensional soil column provides an adequate estimate of the seismic loading in earth slopes. Using the dataset of 144 strong motion pairs of mainshock-aftershock sequences, a total of 720 1D linear equivalent linear site response analyses were performed on five hypothetical sites with site periods of 0.15 s, 0.3 s, 0.48 s, 1 s, and 1.51 s. The details about the configuration of the hypothetical sites are presented by Antonakos [2]. Strata is used to evaluate the dynamic response of flexible sliding masses and specifically to obtain the seismic loading parameters (k_{max}, k-vel_{max}) and k-time history at the base of sliding mass [10]. The k-vel–time histories were obtained by integrating the k–time histories over time.

Next, decoupled sliding displacements were computed using the k-time histories of the aforementioned 720 cases as input for various site and slope conditions. Here, decoupled sliding displacements were calculated for three yield accelerations including 0.04 g, 0.08 g and 0.16 g. Sliding displacements were computed using the SLAMMER program [8]. The maximum decoupled sliding displacements were taken into consideration for the development of the predictive models for flexible slopes subjected to mainshock and aftershock sequences. The resulting dataset consisted of 968 non-zero sliding displacement values for mainshocks and 394 non-zero displacements for recorded aftershocks.

III. Verification of Existing Predictive Models

Rathje and Antonakos [16] developed empirical models for k_{max} and k-vel_{max} using the results of 400 1D site response analyses. These models predict k_{max} and k-vel_{max} as functions of the PGA, PGV and T_m of the input motion and the natural period of the sliding mass (T_s). They extended the (PGA, PGV) rigid sliding displacement model of Saygili and Rathje to make it applicable to flexible sliding masses [20]. The extension involves using k_{max} and k-vel_{max} in place of PGA and PGV in the original (PGA, PGV) vector model, and the addition of the natural period of the sliding mass T_s.

The dataset developed in this research includes a new subset of earthquake strong motion records from the PEER database. This dataset provides a unique opportunity to verify if there is any dataset bias in the predictions of existing predictive models by Rathje and Antonakos [16]. To achieve this objective, empirical relationships are developed for the seismic loading parameters (k_{max} and k-vel_{max}) for verification purposes only to compare the results with the predictions of Rathje and Antonakos [16]. JMP [19] statistical package is used to compute the regression coefficients of k_{max} and k-vel_{max} models.

Fig. 2 shows k_{max}/PGA and k-vel_{max}/PGV as functions of the period ratio (T_s/T_m) for different PGA bins. On average, both k_{max}/PGA and k-vel_{max}/PGV ratios are close to unity at small period ratios. This common trend suggests that sliding masses are acting as rigid bodies at small period ratios. As shown by continuous and dashed lines, the predictions of the models developed in this study are almost coincident with the Rathje and Antonakos models at all PGA levels and period ratios [16]. The comparison of the predictions of two models with different datasets clearly indicates that there is no dataset bias in the predictions of Rathje and Antonakos predictive models [16].

IV. Aftershock Record Selection

There are two common practices to represent the strong motion data for mainshock–aftershock sequences. These are the use of artificial time histories and as-recorded time histories. Artificial time histories are generated by scaling mainshock records as aftershocks. Here, the frequency content and duration characteristics are assumed to be the same. In essence, the ground motion characteristics of the mainshock and aftershocks can be remarkably different than each other. In this section, a case study is presented to illustrate the effects of aftershock selection on earth slopes.

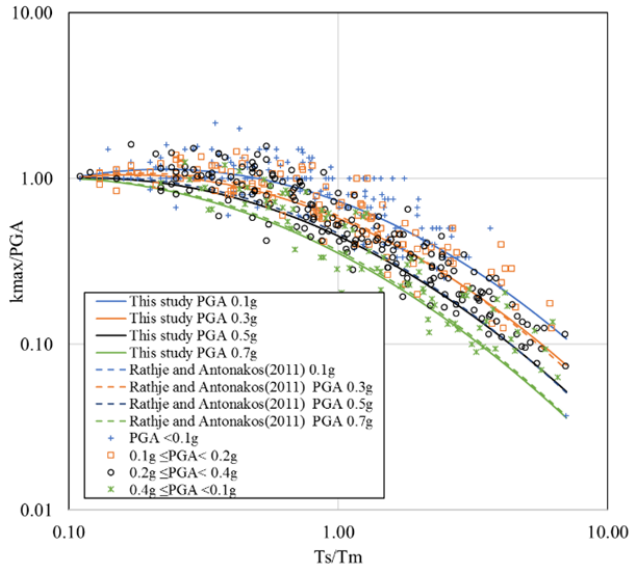

(a)

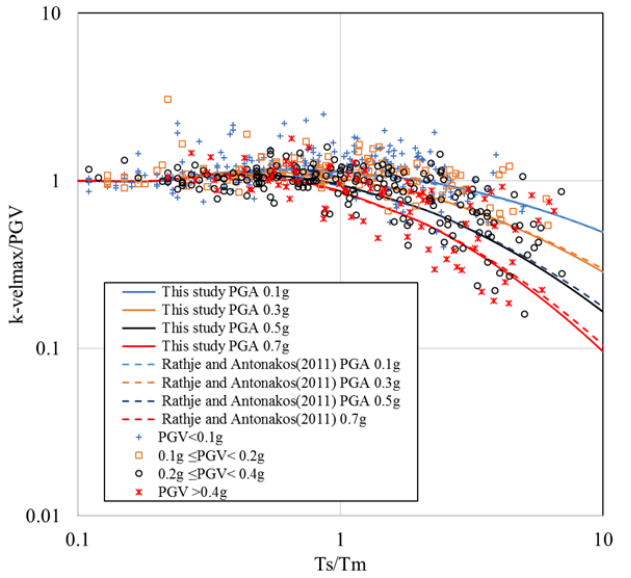

(b)

Fig. 2 Variation of (a) k_{max}/PGA and (b) k-vel_{max}/PGV versus T_s/T_m

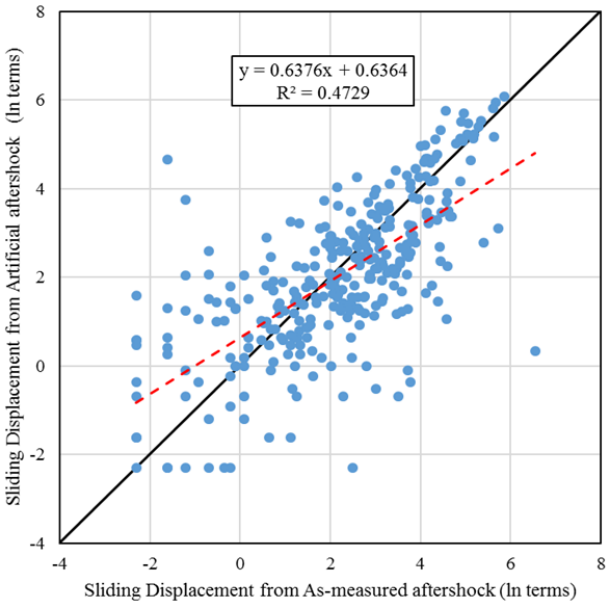

Fig. 3 Decoupled sliding displacements from artificial and as-recorded aftershocks

Decoupled sliding displacements were computed using as-recorded mainshock–aftershock sequences. The mainshocks were then scaled to match aftershocks by the PGV ratio (defined as $PGV_{aftershock}/PGV_{mainshock}$). PGV was selected because it includes some measure of the frequency content of the strong motion due to the numerical integration over time. The scaled mainshocks are labeled as "artificial aftershocks". Decoupled sliding displacements from artificial aftershocks and as-measured aftershocks are presented in Fig. 3. The overall trend of the date (represented by red dashed line) is above the 45-degree line for sliding displacements smaller than 7.5 cm (i.e., lnD = 2) and it is below the 45-degree line for sliding displacements greater than 7.5 cm (i.e., lnD = 2). This inconsistent trend reveals that decoupled sliding displacements from artificial aftershocks can lead to significant overestimation of the seismic demand at small displacement levels and can lead to un-conservative estimation of the seismic demand at large displacement levels. Therefore, as-recorded master mainshock–aftershock sequences were used in this research.

V. Sliding Displacement Models That Incorporate Aftershocks

Various empirical models are available that predict sliding displacement as a function of ground motion parameters and site parameters but the data sets for these empirical models do not accompany aftershock records. The objective of this study is to incorporate the aftershock effects on the recently developed predictive models for flexible sliding masses. Decoupled sliding displacements that consider mainshocks exclusively are used for the investigation of the effects of aftershocks.

Decoupled sliding displacements were calculated using the 720 k-time histories for five site conditions and three yield

acceleration levels (i.e., 0.04 g, 0.08 g, and 0.16 g). The resulting dataset consisted of 968 non-zero sliding displacement values for mainshocks. Rathje et al. presented the sensitivity of predicted k_{max}, k-vel_{max}, and sliding displacement to the site period through a hypothetical case study where the ground shaking is characterized by a M_w = 7, R = 5 km event with PGA = 0.35 g, PGV = 30 cm/s, and T_m = 0.45 s [15]. Here, sliding displacements generally decreased at larger values of site periods as k_{max} decreased. Mainshocks typically cause elongation of the site period of flexible slopes; therefore, it may be assumed that post-mainshock slopes can stay stable following aftershocks as aftershocks exert a relatively low seismic demand on the slope compared to the mainshock. In essence, this assumption is not necessarily correct because post-mainshock slopes can be more fragile when subjected to aftershocks due to the "damage" from the mainshock.

In his third McClelland Keynote Lecture, Andersen introduced a strain-based strength degradation procedure to predict post-mainshock yield accelerations of "damaged" slopes [1]. An assessment of the yield accelerations of post-mainshock slopes is beyond the scope of this research; therefore, a parametric sensitivity is performed to evaluate yield strength degradation. Recent research documented that the friction angle of the post-mainshock slopes are on average are 2% to 8% smaller than those of intact slopes [24], [22], [9]. This observation corresponds to a decrease in the slope yield acceleration by 5% to 20% using an infinite slope approximation. To incorporate the effects of mainshock–aftershock sequences, aftershocks are applied on post-mainshock "damaged" slopes using four levels of yield acceleration reduction factors (i.e., Δk_y = 5%, 10%, 15%, and 20%). The resulting dataset consisted of 394 non-zero displacements for as-recorded aftershocks. As summarized in Table I, average decoupled sliding displacements on post-mainshock slopes subjected to aftershocks increase around 30% at all site periods. Fig. 4 shows that average values of decoupled sliding displacements in aftershock environment increase with an increase in site periods. This decoupled sliding displacement increase is due to the combined effects of strength degradation and the additional seismic demand by the aftershock. Overall, the results suggest that aftershocks increase the seismic demand relative to the mainshock alone; thus, the seismic risk is underestimated if aftershocks are neglected.

TABLE I
PERCENT INCREASE IN DECOUPLED SLIDING DISPLACEMENTS IN AFTERSHOCK ENVIRONMENT

Site Name	Δk_y=5%	Δk_y=10%	Δk_y=15%	Δk_y=20%
Site A	27%	27%	29%	31%
Site B	40%	34%	34%	26%
Site C	34%	36%	35%	36%
Site D	34%	25%	43%	43%
Site E	41%	30%	26%	58%
Overall	**35%**	**30%**	**33%**	**39%**

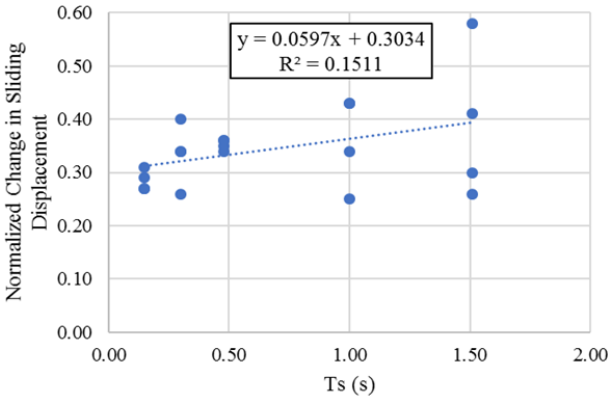

Fig. 4 Decoupled sliding displacement increase due to aftershocks

In an attempt to properly address the aftershock damage, the original flexible sliding displacement models proposed by Rathje et al. [15] are modified to include the strength degradation on the yield acceleration of post-mainshock slopes as follows:

$$lnD = 0.597\mathrm{Ts} + 0.3034 + 4.89 - 4.85\left(\frac{k_y}{k_{max}}\right) - 19.64\left(\frac{k_y}{k_{max}}\right)^2 + 42.49\left(\frac{k_y}{k_{max}}\right)^3 - 29.06\left(\frac{k_y}{k_{max}}\right)^4 + 0.72\ln(k_{max}) + 0.89(\mathrm{M}-6) + \begin{cases} 3.69 \cdot T_s - 1.22.\,\mathrm{Ts}^2 & T_s \le 1.5\ s \\ 2.78 & T_s > 1.5\ s \end{cases} \quad (1)$$

$$lnD = 0.597\mathrm{Ts} + 0.3034 - 1.56 - 4.58\left(\frac{k_y}{k_{max}}\right) - 20.84\left(\frac{k_y}{k_{max}}\right)^2 + 44.75\left(\frac{k_y}{k_{max}}\right)^3 - 30.50\left(\frac{k_y}{k_{max}}\right)^4 - 0.64\ln(k_{max}) + 1.55\ln(k - vel_{max}) + \begin{cases} 1.42 \cdot T_s & T_s \le 0.5\ s \\ 0.71\ T_s & T_s > 0.5\ s \end{cases} \quad (2)$$

where D is displacement in cm, M is the magnitude, k_y is the yield acceleration in g, and k_{max} and k-vel_{max} are seismic shaking parameters in units g and cm/sec, respectively. (1) is the decoupled sliding displacement equation for the scalar (k_{max}, M) model and (2) is the decoupled sliding displacement equation for vector (k_{max}, k-vel_{max}) model.

VI. CASE STUDY

Two hypothetical 30-m slopes with average shear velocities of Vs = 400 m/s (Site B) and Vs = 250 m/s (Site C) were considered. The resulting site periods are 0.3 s for Site B and 0.48 s for Site C ($T_s = 4H/V_s$). Four seismic events with M_w = 6.5, 7.0, 7.5, and 8 are considered. Widely used ground motion prediction models are used to calculate PGA and PGV [3] and T_m [15]. For the T_m prediction, the closest distance from the epicenter to the site is assumed as 10 km. Table II provides a summary of the expected ground motion parameters for various seismic events at Site B and Site C. As expected, both PGA and PGV increase with the increase in earthquake magnitude.

Seismic loading parameters (k_{max} and k-vel_{max}) are computed using the ground motion parameters and site characteristics summarized in Table II. Table III shows the predicted decoupled sliding displacement values for flexible

sliding masses with yield acceleration of 0.1 g in mainshock only and aftershock environments. On average, the increase in decoupled sliding displacement when subjected to mainshock–aftershock sequence is around 30.9% for the scalar (k_{max}, M) model and 31.3% for the vector (k_{max}, k-vel_{max}) model.

Fig. 3 shows the predictions of the sliding displacement models for mainshock only and mainshock–aftershock sequence for site B at three yield accelerations including k_y=0.1g, 0.15 g, and 0.2 g. In accordance with the previous observations, aftershocks increase seismic demands relative to the mainshock alone; thus, the seismic risk may be underestimated if aftershocks are neglected.

TABLE II
SUMMARY OF THE PREDICTED GROUND MOTION PARAMETERS [3], [15]

Site Class	Magnitude	PGA (g)	PGV (cm/s)	T_m (s)	T_s/T_m
Site B ($V_{s,30}$ = 400 m/s)	6.5	0.27	26.54	0.51	0.59
	7.0	0.31	35.35	0.56	0.54
	7.5	0.36	47.05	0.58	0.52
	8	0.41	62.62	0.58	0.52
Site C ($V_{s,30}$ = 250 m/s	6.5	0.29	32.07	0.51	0.94
	7.0	0.32	41.92	0.56	0.86
	7.5	0.36	54.74	0.58	0.82
	8	0.40	71.40	0.58	0.82

TABLE III
DECOUPLED SLIDING DISPLACEMENT VALUES FOR FLEXIBLE SLIDING MASSES WITH K_Y = 0.1 G IN MAINSHOCK ONLY AND AFTERSHOCK ENVIRONMENT

Parameter	k_{max} (g)	k-vel_{max} (cm/s)	D (k_{max}, M) model (cm)		D (k_{max}, k-vel_{max}) model (cm)	
Seismic Environment	-	-	MS only	MS-AS	MS only	MS-AS
Site B (V_{s30}=400m/s)	0.21	29.89	5.10	7.29	5.87	8.22
	0.25	39.60	14.68	18.34	13.60	17.13
	0.28	52.41	34.32	39.83	27.16	32.08
	0.31	69.16	71.86	79.73	50.06	56.67
Site C (V_{s30}=250m/s)	0.17	33.85	3.23	5.23	3.67	5.82
	0.20	44.40	9.21	12.92	8.56	12.11
	0.22	57.64	21.45	27.56	16.85	22.14
	0.23	74.04	42.92	52.10	29.30	36.64

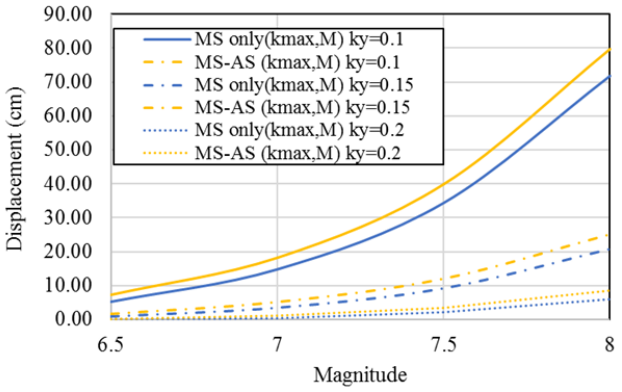

(a)

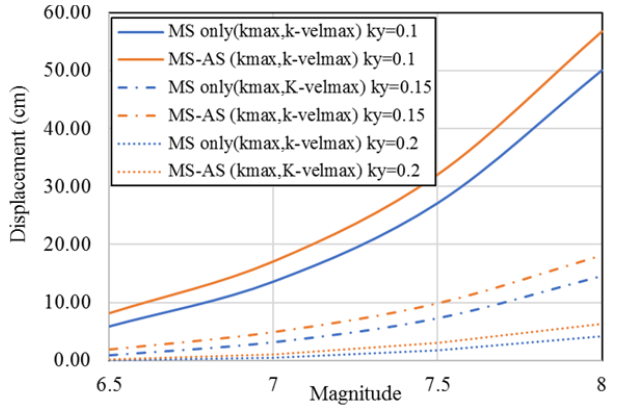

(b)

Fig. 5 Decoupled sliding displacements in mainshock only and aftershock environments as a function of earthquake magnitude using the (a) k_{max}, M model and (b) k_{max}, k-vel_{max} model (Site B)

VII. CONCLUSIONS AND DISCUSSIONS

This study provides an improved assessment of the risks associated with the seismic performance of slopes subjected to mainshock–aftershock sequences. Post-mainshock slopes can experience delayed failures due to undrained creep. Aftershocks can simply trigger the failure as there is not enough time for repair and retrofit between mainshock–aftershock sequences. Seismic stability analyses of earth slopes should account for mainshock–aftershock sequences.

Obtained from the PEER resources, a comprehensive dataset with strong ground motion records from a total of 144 mainshocks and their corresponding aftershocks were used in this study. As-recorded aftershocks were used in this research because a comparison of the resulting seismic demand parameters for earth slopes revealed that artificial aftershocks can lead to significant overestimation of the seismic demand parameters at relatively small displacement levels and unconservative estimation at relatively large displacement levels. The dataset developed in this research included a new subset of earthquake strong motion records from the PEER database. Hence, it is used to demonstrate that there is no dataset bias in the predictions of Rathje and Antonakos predictive models [16].

Using the k-time histories generated for various site conditions, decoupled sliding displacements were computed for mainshocks and aftershocks. Decoupled sliding displacements of post-mainshock slopes subjected to aftershocks were predicted by applying yield acceleration reduction factors to account for the strength degradation caused by the mainshock. The resulting decoupled sliding displacement dataset consisted of 394 non-zero sliding displacement values for aftershocks. A comparison of the mainshock only and mainshock–aftershock cases suggested

that decoupled sliding displacements on post-mainshock slopes subjected to aftershocks increased on average around 30% at all site periods. The original decoupled sliding displacement predictive models for flexible slopes proposed by Rathje et al. [15] are modified to incorporate the effects of aftershocks. These models predict the sliding displacement as a function of ground motion parameters and site parameters.

The failure of post-mainshock slopes is due to the combined effects of strength degradation and the additional seismic demand by aftershocks. Overall, the results suggested that aftershocks increase the seismic demand relative to the mainshock alone; thus, the seismic risks are underestimated if aftershocks are neglected.

REFERENCES

[1] Andersen, K. H. (2015). Cyclic soil parameters for offshore foundation design. Frontiers in Offshore Geotechnics III.

[2] Antonakos, G. 2009. Models of Dynamic Response and Decoupled Displacements of Earth Slopes during Earthquakes. PhD Thesis, Austin, Tx: University of Texas at Austin.

[3] Boore, M. B., Stewart P. J., Seyhan E., and Atkinson M. G. 2014. "NGA-West 2 Equations forPredicting PGA, PGV, and 5% Damped PSA for Shallow Crustal Earthquakes." Earthquake Spectra 1057-1085.

[4] Chiou, B., Darragh, B., & Power, M. (2005). NGA Documentation. Nation Geospatial-Intelligence Agency (NGA).

[5] Goda, K. 2014. "Record selection for aftershock incremental dynamic analysis." Earthquake Engineering and Structural Dynamics.

[6] Han, R., Y. Li, and J. Lindt. 2014. "Seismic risk of base isolated non-ductile reinforced concrete buildings considering uncertainties and mainshock-aftershock sequences." Structural Safety 39-56.

[7] Jeon, J., R. DesRoches, L. N. Lowes, and I. Brilakis. 2015. "Framework of aftershock fragility assessment–case studies: older California reinforced concrete building frames." Earthquake Engineering and Structural Dynamics.

[8] Jibson, R. W., E. M. Rathje, M. W. Jibson, and Y. W. Lee. 2013. Seismic Landslide Movement Modeled using Earthquake Records. Software Manual, United States Department of the Interior, United States Geological Survey.

[9] Kim, C., Smell, C., & Medley, E. (2004). Shear Strength of Franciscan Complex Melange as Calculated from Back-Analysis of a Landslide. Geotechnical Engineering Commons. Missouri: Missouri University of Science and Technology Scholar's Mine.

[10] Kottke, A. R., & Rathje, E. M. (2009). Technical Manual for Strata. California: Pacific Earthquake Engineering Reseach Center.

[11] Li, Y., R. Song, and J. W. Van De Lindt. 2014. "Collapse Fragility of Steel Structures Subjected to Earthquake Mainshock-Aftershock Sequences." Journal of Structural Engineering 140(12) Collapse Fragility of Steel Structures Subjected to Earthquake Mainshock-Aftershock Sequences.

[12] PEER Ground Motion Database. (2014). Retrieved 2018, from https://ngawest2.berkeley.edu/.

[13] Raghunandan, M., Liel, A. B., & Luco, N. (2015). Aftershock collapse vulnerability assessment of reinforced concrete frame structures. Earthquake Engineering & Structural Dynamics, 44(3), 419-439.

[14] Rathje, E. M., and J. D. Bray. 2001. "One- and two-dimensional seismic analysis of solid-waste landfills." Canadian Geotechnical Journal, 38 850-862.

[15] Rathje, E. M., Wang, Y., Stafford, P. J., Antonakos, G., & Saygili, G. (2014). Probabilistic assessment of the seismic performance of earth slopes. Bulletin of Earthquake Engineering, 12(3), 1071-1090.

[16] Rathje, E. M., & Antonakos, G. (2011). A unified model for predicting earthquake-induced sliding displacements of rigid and flexible slopes. Engineering Geology, 122(1-2), 51-60.

[17] Ruiz-García, J., and J. C. Negrete-Manriquez. 2011. "Evaluation of drift demands in existing steel frames under as-recorded far-field and near-fault mainshock–aftershock seismic sequences." Engineering Structures 621-634.

[18] Ruiz-Gracia, J., and J., D. Aguilar. 2017. "Influence of modeling assumptions and aftershock hazard level in seismic response of post-mainshock steel framed buildings." Engineering Structures, 140 437-446.

[19] SAS. 2018. "JMP." Computer Software.

[20] Saygili, G., and E. M. Rathje. 2008. "Empirical Predictive Models for Earthquake Induced Sliding Displacement of Slopes." Journal of Geotechnical and Geoenvironmental Engineering 790-803.

[21] Song, R., Y. Li, and J. W. Van de Lindt. 2014. "Impact of earthquake ground motion characteristics on collapse risk of post-mainshock buildings considering aftershocks." Engineering Structures.

[22] Tiwari, B., Brandon, L. T., Marui, H., & Tuladhar, R. G. (2005). Comparison of Residual Shear Strengths from Back Analysis and Ring Shear Tests on Undistrurbed and Remodeled Specimens. ASCE.

[23] Vrymoed, J. L., and E. R. Calzascia. 1978. "Simplified determination of dynamic stresses in earth dams." Earthquake Engineering and Soil Dynamics. New York: ASCE. 991-1006.

[24] Wu, J.-H., & Tsai, P.-H. (2011). New dynamic procedure for back-calculating the shear strength parameters of large landslides. Engineering Geology 123, 129-147.

[25] Yin, Y., J., and Y. Li. 2010. "Seismic collapse risk of light-frame wood construction considering aleatoric and epistemic uncertainties." Structural Safety 32(4) 250-261.